



Full length article

Exposure to nanoplastics exacerbates light pollution hazards to mammalian

Haipeng Huang ^{a,b,c}, Jiaqi Hou ^{a,*} Yilie Liao ^d, Jing Yu ^{b,c}, Beidou Xi ^{a,*}^a State Key Laboratory of Environment Criteria and Risk Assessment, Chinese Research Academy of Environmental Sciences, Beijing 100012, China^b Institute of Molecular Medicine, College of Future Technology, Peking University, Beijing 100871, China^c Research Unit of Mitochondria in Brain Diseases, Chinese Academy of Medical Sciences, PKU-Nanjing Institute of Translational Medicine, Nanjing 210061, China^d Duke-NUS Medical School, National University of Singapore, Singapore 169857, Republic of Singapore

ARTICLE INFO

Handling Editor: Adrian Covaci

Keywords:

Nanoplastic
Circadian rhythm
Mouse
Bmal1
Light contamination
Health

ABSTRACT

Environmental light pollution adversely affects brain function, disturbing circadian rhythms and negatively impacting human health. Nanoplastics (NPs) pollution is pervasive in the human environment, and their minuscule size facilitates entry into the body, particularly invading brain and compromising its functionality. However, whether NPs infiltrate rhythm-regulated brain regions and disrupt circadian rhythms in organisms remains unclear. Our study demonstrates that exposure to NPs in mice perturbs normal circadian rhythms. Specifically, NPs invade the suprachiasmatic nucleus (SCN), affecting the circadian clock genes network and altering the regular oscillations of core clock genes. Exposure to NPs renders the intrinsic rhythms more susceptible to disruption by light pollution, resulting in more pronounced disorder to metabolism, immune regulation, and brain function. This work is the first to investigate the combined effects of ambient light pollution and NPs pollution on mammalian health, and our findings suggest that NPs amplify the health impacts of light pollution. These findings also highlight that efforts to mitigate human health risks from environmental pollutants should begin to consider the synergistic effects of various classes of pollutants.

1. Introduction

The global production of plastics and plastic waste generation has been increasing annually. Many plastic pollutants have undergone physical or chemical transformations to form microplastics (MPs, 1 µm–5 mm) and nanoplastics (NPs, less than 1 µm) (Rillig and Lehmann, 2020, Gigault et al., 2018). These plastic particles accumulate in the environment and infiltrate the human habitat and food chain, leading to unavoidable human exposure and subsequent accumulation in bodily tissues (Vethaak and Legler, 2021, Lin et al., 2022, Wright and Kelly, 2017). Compared to MPs, NPs exhibit biological effects related to their size due to their smaller dimensions and enhanced ability to diffuse after penetrating tissues (Jiang et al., 2008, Pastore, 2021, Huang et al., 2023). Therefore, understanding the role and hazards of NP exposure on the health of living organisms is crucial. Several studies using rodent models have shown that NPs can be detected in various organs following exposure (Ding et al., 2021, Lu et al., 2022). Moreover, it has been observed that NPs accumulate at a relatively high level in the brain (Liang et al., 2024, Zhang et al., 2024). NPs induce metabolic disorders, oxidative stress, and reduced reproductive capacity in these tissues (Banerjee and Shelver, 2021). Importantly, NPs have the potential to

cross the blood–brain barrier (BBB), thereby entering the mammalian brain (Jeong et al., 2022, Zou et al., 2024).

Studies showed NPs cross the BBB following intestinal absorption and blood transportation, subsequently impacting neurodevelopment and neuromodulation (Zou et al., 2024, Liang et al., 2024, Ze et al., 2014). This intrusion may lead to abnormal neurobehavioral activities, such as mood alterations in mice. Furthermore, mouse experiments indicate that NPs present in brain tissue are believed to induce and exacerbate the pathological spread of neural α-synuclein aggregates, potentially contributing to the development of Parkinson's disease (Liang et al., 2022, Liu et al., 2023).

Moreover, urban light pollution, resulting from excessive or inappropriate artificial light sources, poses a prevalent environmental challenge in modern urbanization (Zielinska-Dabkowska et al., 2023, Cao et al., 2023). Beyond being a waste of energy, light pollution adversely affects both ecosystems and human health. Excessive illumination disrupts human circadian rhythms and compromises sleep quality, which can lead to metabolic disorders, reduced immunity, and increased susceptibility to various diseases (Cao et al., 2023, Tähkämö et al., 2019, Smolensky et al., 2015). The suprachiasmatic nucleus (SCN) in the brain serves as the central organ for regulating biological rhythms in response

* Corresponding authors.

E-mail addresses: houjiaqi0325@163.com (J. Hou), xibd@craes.org.cn (B. Xi).

to light signaling (Dibner et al., 2010). However, the effects of current environmental pollutants, particularly NPs, on biological rhythms in the brain remain unclear. Given the widespread prevalence of light pollution, it is essential to investigate the health impacts of NP exposure on urban populations affected by light pollution.

This study aimed to investigate the impact of NPs on physiological rhythms in mice and to assess the health effects of NPs in the context of light pollution. Our findings demonstrate that polystyrene NPs can disrupt physiological rhythms in mice. In experiments examining rhythm disturbances induced by light pollution, exposure to NPs led to multiple physiological and neurobehavioral abnormalities. This study is the first to integrate the hazards of environmental light pollution with the neurological effects of NPs in a comprehensive experimental framework. It offers a novel perspective for understanding the exposure risks of NPs in humans under urban light pollution conditions.

2. Materials and methods

2.1. Animal husbandry

All the animal husbandry and experimental procedures were in strict accordance with the guidelines approved by the Institutional Animal Care and Use Committee (IACUC) (Approval ID: PA23053002-0) of Charles River. All the mice were housed in a specific pathogen-free (SPF) facility at Charles River Laboratory Animal Research Center under a 12/12-hour light–dark cycle and controlled temperature ($25 \pm 1^\circ\text{C}$) with free access to water and food. Mice were kept in strict accordance with the International Genetic Standardization.

Wild-type (WT) C57BL/6J mice were procured from Vital River Laboratory. The SCN-tagged mice expressing GCaMP6f specifically in GABAergic neurons (*Viaat-Cre::GCaMP6f* mice) were generated by crossing *Viaat-Cre* mice (JAX #017535) with *Rosa26-LSL-GCaMP6f* mice (JAX #024105). The NPs exposure experiments were conducted using WT mice, male instead of female to mitigate the potential confounding effects introduced by metabolism-related hormonal regulation in females, thereby enhancing the precision of the results. We utilized 200 nm diameter polystyrene nanoplastic (PS-NP) spheres (Base Line Chrom Tech Research Centre, Tianjin, China, Cat#7-3-0020). Exposure to NPs was conducted by adding NPs to the mice's drinking water instead of a direct gastric gavage, beginning at 12 weeks of age. The specialized drinking water mixed with NPs should be stored in glass drinking bottles. Furthermore, the bottle was shaken periodically during feeding to ensure thorough mixing of the NPs. Considering the daily water intake of mice, we established three treatment concentrations for the NPs in drinking water: 0.1 $\mu\text{g}/\text{mL}$, 1 $\mu\text{g}/\text{mL}$, and 10 $\mu\text{g}/\text{mL}$. Considering the 3.5 mL daily water intake, these are approximated NPs exposure levels of 0.0098 mg (NPs)/kg (mouse body weight), 0.098 mg/kg, and 0.98 mg/kg. This approach will render the results comparable to previously reported studies (Zou et al., 2024, Liang et al., 2024, Ze et al., 2014, Senathirajah et al., 2021). Detailed information regarding the administration of NP exposure and mouse arrangements can be found in the Supplementary Material (Figs. S1, S5, S10).

2.2. Arrangements for exposure of NPs in mice

Considering that the primary test index of this experiment is the circadian rhythm of the animals, accurate testing necessitates minimizing the interference of external factors on the experimental subjects to prevent any impact on the results of behavioral experiments. Gavage administration in mice poses a potential risk of altering their hormone levels and inducing anxiety and inflammation (Larcombe et al., 2019, Miguelena Chamorro et al., 2023, Huang et al., 2023). Thus, exposure to NPs was conducted by adding NPs to the mice's drinking water. The bottles were shaken periodically during feeding to keep a thorough mixing of the NPs.

We reference previous research on mouse exposure to NPs, a dose of

2.5 mg (NPs)/kg (mouse body weight) was acceptable using mouse exposure (Zou et al., 2024, Liang et al., 2024, Ze et al., 2014, Zhang et al., 2023, Mohamed Nor et al., 2021, Senathirajah et al., 2021). Regarding potential MPs exposure levels in humans, an assessment of potential human exposure to microplastics (MPs) indicates that the exposure level for a 70 kg adult is approximately 0.2–10 mg (MPs)/kg (human body weight)/day (Senathirajah et al., 2021). Another comparable assessment yielded somewhat smaller results, ranging about 0.58 ng (MPs)/kg (human body weight)/day (Based on a body weight of 70 kg) (Mohamed Nor et al., 2021). A consideration is that only nanoscale plastics can cross the blood–brain barrier and enter the brain. Therefore, in addition to the aforementioned research background, it is crucial to give further attention to the potential levels of human exposure specific to NPs. Bottled drinking water is a daily necessity frequently utilized by individuals. The estimated annual exposure of NPs through bottled drinking water is approximately 1×10^{14} particles, based on a daily water intake of 2 L for adults (Zhang et al., 2023). If the calculation is also based on a body weight of 70 kg, it would be 1.4×10^{12} particles/kg. And exposure to NPs through contaminated water is merely one of the numerous potential sources of NPs exposure.

However, it is important to note that this analysis only considered potential exposure to NPs through ingestion sources through a traditional way. Considering the complexity of human life scenarios, lifestyle habits are likely to have a direct impact on the level of exposure to NPs. For instance, Hussain et al. (Hussain et al., 2023) reported that certain containers could release 2.1×10^9 NPs particles from just one square centimeter of plastic area within three minutes of microwave heating. Consequently, consuming a microwave-warmed bag of milk packaged in plastic may result in the intake of at least 1×10^{11} NPs.

We established three treatment concentrations for the NPs in drinking water: 0.1 $\mu\text{g}/\text{mL}$, 1 $\mu\text{g}/\text{mL}$, and 10 $\mu\text{g}/\text{mL}$. By applying a particle density of 1.064 g/cm^3 , we determined a presumed daily exposure level of 2.2×10^9 particles/kg in mice at our lowest NPs treatment concentration. However, given that the duration of human exposure to NPs could span decades (much longer than the treatment period for mice) it is important to consider their continuous cumulative effects.

2.3. A light-induced circadian disruption in mice

Based on a previously reported study (Karatsoreos et al., 2011), we employed a classical light-induced circadian dysregulation model in mice with certain modifications. Briefly, the mice were housed in a room with programmable lighting. The light exposure duration was maintained at 12 h, but the onset of illumination was shifted every two days, with each shift occurring six hours earlier. Consequently, the starting time of illumination was altered three times over a period of eight days. After these three changes, the light rhythm returned to the initial setting. We subjected the mice to six light-induced cycles over a total duration of 48 days. At the conclusion of the experiment, the mice were kept under the final light setting, and additional experimental tests were conducted.

2.4. Metabolic cage detection of mouse circadian rhythm

Metabolic cage (CLAMS, Columbus Instruments, Columbus, USA) was placed in a light-regulated separate room. No other experiments were conducted in this room, and personnel were not permitted to remain for extended periods during the entire experiment. Each mouse was housed in an individual cage for detection experiments. To accurately assess the behavioral rhythms of the mice, it is essential to minimize the influence of external factors. Mice in each group were generally acclimatized to the room environment by being kept in a single cage for 2 days before the experiment. For circadian rhythm detection experiments, the duration of each experiment typically spans 4 days. The initial 2 days serve as the environmental acclimatization period, and data collected during this time should not be included in

subsequent analyses. Data analysis is conducted using a complete 24-hour circadian cycle from days 3 to 4. The device records mouse locomotion data every 7 min. For statistical analysis, the total amount of exercise for each mouse over the course of one hour is aggregated.

2.5. Preparation of SCN

The mice were anesthetized with 1.25 % tribromoethanol (MeilunBio, Cat#MA0478-2) and subsequently transcardially perfused with ice-cold artificial cerebrospinal fluid (aCSF) (110 mM choline chloride, 25 mM NaHCO₃, 25 mM D-glucose, 7 mM MgCl₂·6H₂O, 2.5 mM KCl, 1.3 mM NaH₂PO₄, 0.5 mM CaCl₂, 1.3 mM L-sodium ascorbate and 0.6 mM sodium pyruvate at pH 7.4) for sectioning. Following this, the mice were decapitated, and the brains were removed. The optic nerves were carefully severed to prevent any stretching that could damage the SCN. The brains were then rapidly immersed in ice-cold aCSF and sliced using a vibratome, with sections ranging from Bregma -0.12 mm to Bregma -0.92 mm. An 800-μm coronal slice containing the SCN was prepared and placed on a glass slide, with aCSF added dropwise to maintain moisture. By identifying the SCN region in the *Viaat-Cre::GCAMP6f* mice, the morphological location of the SCN in the slice was distinguished and marked. Subsequently, the SCN region was carefully excised and isolated using a glass tube.

2.6. Py-GCMS detection of plastics in tissue

Biological tissue samples were placed into glass vials rinsed with ultrapure water and either immediately processed for the next step of the experiment or stored temporarily at -20°C. Prior to thermal lysis, the samples needed to be dried to a constant weight, and their mass accurately measured. A specific mass of the weighed sample was placed into the reactor, to which 10 ml of the extraction solution was added. The reaction was conducted for 10 min while ultrasonication was applied. The reacted extract was then transferred to another beaker. This process was repeated five times by reintroducing a new extraction solution into the reactor. After the final addition of the extract, the mixture was heated at 150°C for 10 min and subsequently combined with the previously collected extract, resulting in a total volume of 70 ml. These extracts were concentrated on a heated plate at 90°C to less than 1 g for the samples to be assayed, which were then prepared for loading. The sample was added to the injector of the pyrolysis-gas chromatography-mass spectrometry (pyr-GC/MS) and concentrated at 90°C on a heated plate until completely evaporated. The samples were analyzed using Py-GCMS (Shimadzu, Kyoto, Japan, Cat#QP2020NX). Standards with varying concentrations were prepared and tested by Py-GCMS to construct a quantitative curve for determining the plastic content in the tissue.

2.7. Quantitative reverse transcribed polymerase chain reaction (qRT-PCR)

Total RNA was extracted using TRIzol reagent (Invitrogen) according to the manufacturer's recommendations. The mRNAs were reverse transcribed using the FastKing RT Kit (Tiangen, Cat#KR116). Quantitative PCR was performed using the EvaGreen Mastermix on an Applied Biosystems StepOne or Vii7 Real-Time PCR System (Applied Biosystems, Foster City, CA, USA). Duplicate runs of each sample were normalized to *36b4* to determine the relative gene expression levels. Sequence information for the primers is provided within the [Supplementary Material \(Table S1\)](#).

2.8. Protein extraction and western blot analysis

The SCN tissues were placed in liquid nitrogen and subsequently stored at -80 °C. A unilateral tissue block of the SCN was used for protein lysate extraction. Each tissue sample was extracted using 150 μL

of ice-cold radioimmunoprecipitation assay (RIPA) lysis buffer (50 mM Tris pH 7.5, 150 mM NaCl, 0.1 % SDS, 1 % NP-40, 0.5 % sodium deoxycholate) supplemented with protease and phosphatase inhibitor cocktails (Pierce, Cat#78441). The lysates were clarified by centrifugation at 13000 rpm for 15 min, and protein concentrations were quantified by BCA (Solarbio, Cat#PC0021). Equal amounts (40 μg) of tissue lysates were resolved by SDS-PAGE, blotted onto a nitrocellulose membrane (Pall, Cat#66485), blocked with 5 % milk in TBST for 1 h at room temperature, incubated overnight with primary antibodies at 4 °C. The blots were then washed and incubated with HRP-conjugated secondary antibody for 1 h at room temperature, and visualized by ECL (Merck Millipore, Cat#WBKL50500) using a ChemiDoc MP imaging system (BioRad). For the detection of phosphoepitopes, BSA instead of milk was used for blocking and antibody preparation.

2.9. Circadian rhythm oscillation analysis

The circadian rhythm oscillation analysis software, Circacompare (<https://github.com/RWParsons/circacompare>), was employed to investigate the fluctuation characteristics (mesor, amplitude, phase) of circadian clock genes and proteins (Parsons et al., 2020).

2.10. Blood monocyte level measurement

At 7 AM, 3 PM, and 11 PM, approximately 200 μL of fresh retro-orbital blood was collected from the mice using capillary tubes and transferred into EDTA tubes. Blood was thoroughly mixed in the tube, and the measurement was supposed completed within two hours. The blood monocyte level was measured using the iDexx Procyte Dx* Hematology Analyzer (iDexx Laboratories Inc., Westbrook, ME, USA).

2.11. Measurements of glucose and FFAs in the serum

The fresh blood was collected from the orbits of the mice using capillary tubes. Immediately test blood glucose utilizing a glucose meter (Zhuoyue, Roche Diabetes Care GmbH, USA). EDTA tubes were utilized to receive other 500 μL of fresh blood samples. The blood was allowed to stand for 1 h at room temperature, then centrifuged at 4°C at 3,500 rpm for 15 mins, and the supernatant was collected on ice or in 4°C for the subsequent assay steps. Serum FFAs were measured using Kits (Sangon Biotech, Cat#D799794) according to the manufacturer's protocol.

2.12. Serum immune factor test

The fresh blood was collected from the orbits of the mice using capillary tubes. EDTA tubes were utilized to receive approximately 700 μL of fresh blood samples. The blood was centrifuged within 2 h post collection, 4°C at 13,000 rpm for 15 mins, and the supernatant was collected for the subsequent assay steps. Serum IL6, IFN-γ, and TNF-α levels were measured using Kits (Sangon Biotech, Cat#D721022 / Cat#D721025 / Cat#D721217) according to the manufacturer's protocol.

2.13. ROS detection in animal tissue

The Tissue Reactive Oxygen Species (ROS) test kit (DHE) (Baiao Laibo, Cat#HR8821) was utilized for this experiment. Fresh tissue samples were rinsed with PBS. A precise weight of 50 mg of tissue was measured, and 1 mL of homogenization buffer A was added before thoroughly homogenizing the mixture. The homogenate was then centrifuged at 100 × g for 3 min at 4 °C. The precipitate was discarded, and the supernatant was collected. Subsequently, 200 μL of the homogenization supernatant and 2 μL of the DHE probe were added to a 96-well plate and mixed thoroughly. The plate was incubated in the dark at 37 °C for 15 to 30 min. Fluorescence intensity was measured using a fluorescence enzyme marker, with excitation at wavelengths of

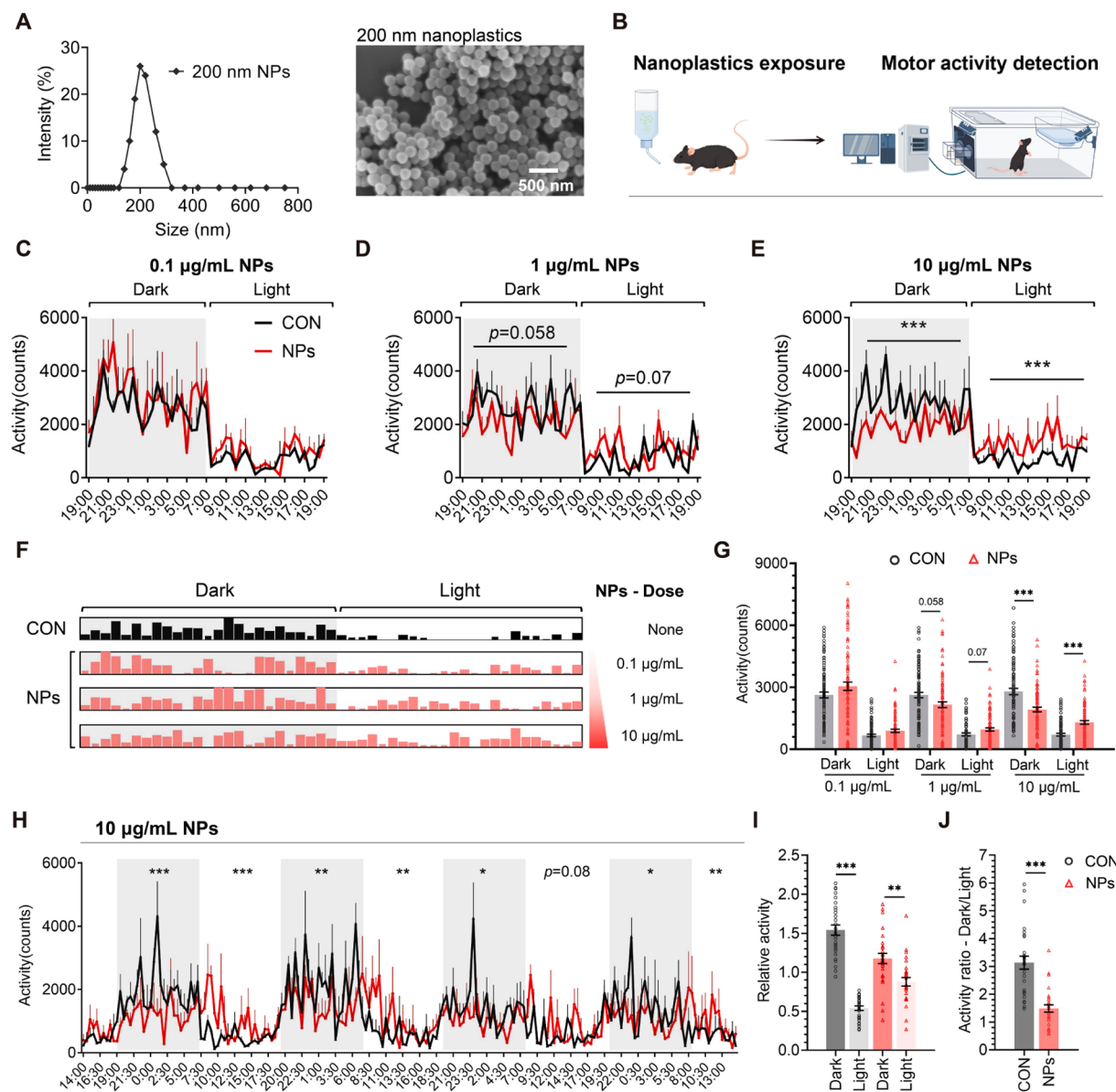


Fig. 1. PS-NP exposure causes circadian rhythm disruption in mice. (A) Characterization of nanoplastic particles utilized in experiments, size distribution and scanning electron microscope micrograph. (B) Schematic diagram depicting activity rhythm monitoring in mice. (C-E) Circadian rhythm detections and metabolic cages were utilized to detect circadian activity in control (CON) and NPs-exposed (NPs) mice, $n = 6$ mice for each group. 3 NPs concentrations were used, 0.1 $\mu\text{g/mL}$ (C), 1 $\mu\text{g/mL}$ (D), 10 $\mu\text{g/mL}$ (E). (F) Representative 24-hour activity distribution of mice. (G) A comparative analysis of the activity levels of each group of mice during the dark and light phases. (H-J) Activity detection in mice subjected to multiple photoperiods in 10 $\mu\text{g/mL}$ NPs exposed group (H). A comparative analysis of the relative levels of activities during the dark and light phases (I). Diurnal activity ratio in mice (J). Data are represented as mean \pm SEM. * $P < 0.05$, ** $P < 0.01$, and *** $P < 0.001$.

488–535 nm and emission at 610 nm. An additional 50 μL of the supernatant homogenate was taken and diluted approximately 30-fold with PBS, and 100 μL was used for protein quantification. The protein concentration data were employed as a correction factor to standardize the homogenization of different samples.

2.14. Open field test

The dimensions of the open field for the mice are 50 cm in length, 50 cm in width, and 40 cm in height. The laboratory environment is maintained in a quiet state with controlled lighting at a moderate level. Prior to the experiment, the mice were acclimatized to the laboratory environment for at least 30 min to minimize stress response to the unfamiliar surroundings. At the start of the experiment, the mice were gently placed in a corner of the open field, with each mouse starting

from the same initial position. The behavioral activities of the mice were recorded via filming for a duration of 7 min. After the completion of the experiment for each mouse, any residual urine in the experimental area was cleaned using alcohol. Following the cleanup, the alcohol odor was allowed to dissipate before proceeding with the next mouse.

2.15. Y maze

The Y-maze consisted of a Y-shaped compartment ($21 \times 7 \times 15.5$ cm), it is three arms of equal length. The mice were acclimated to the laboratory environment for 3 days before the experiment to familiarize themselves with the room and reduce stress. The arms of the maze were labeled A, B, and C. Mice were gently placed in the fixed arm facing the center of the maze. They were given 8 min to explore the maze freely. The maze was thoroughly cleaned with alcohol between experimental

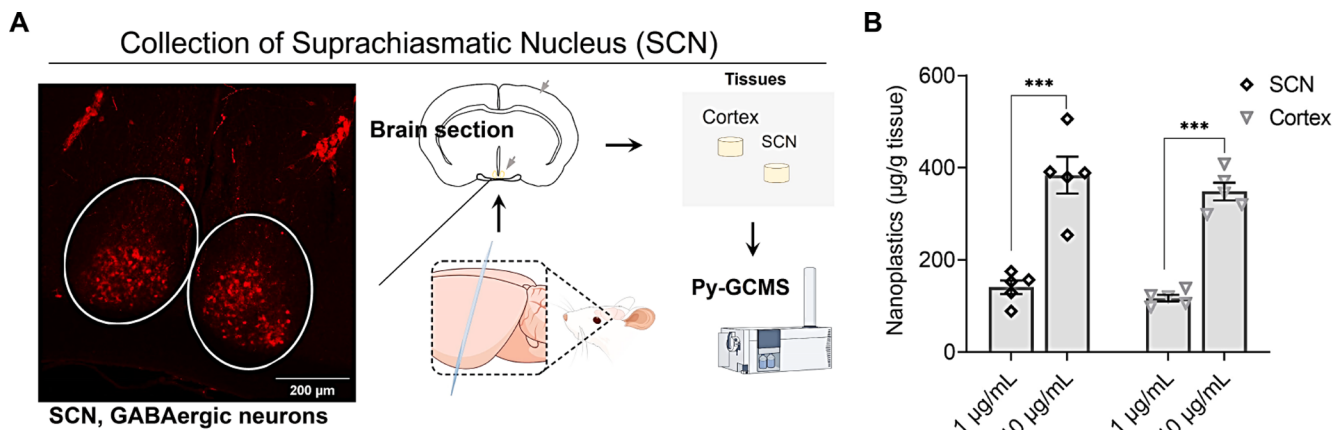


Fig. 2. Identification of NPs in SCN in Mice. (A) Schematic representation of the tissue sampling and plastic identification. (B) Plastic content within the tissue in the control, 1 $\mu\text{g}/\text{mL}$ and 10 $\mu\text{g}/\text{mL}$ NPs-exposed groups ($n = 5$ for each group). Data are represented as mean \pm SEM. *** $P < 0.001$.

mice.

$$\% \text{ alternations} = \frac{\text{total number of alternations}}{\text{number of arms entered}} \times 100 \%$$

2.16. Statistical analysis

Student's unpaired *t*-test was performed to determine statistical differences between the two groups. *P*-values of less than 0.05 were considered as significant. *P*-values greater than 0.05 and less than 0.1 are annotated in the figure. *N* denotes the number of biological replicates in each experiment, and it is provided in the corresponding figure legends. Immunoblot quantification was completed by AlphaView (FluroChem FC3). The schematics presented in Figs. 1, 2, 4, 6, and 8 were created by Haipeng Huang using Figdraw (<https://www.figdraw.com/static/index.html#/>). All graphs were drawn in Graphpad Prism 8.0.2 software.

3. Result and discussion

3.1. PS-NP exposure causes circadian rhythm disruption in mice

The normal circadian rhythmic regulation of rodents, influenced by their inherent habits, leads them to engage in behavioral activities during the dark phase and to rest and sleep during the bright phase during a 24-hour light cycle. We aimed to investigate the impact of NPs exposure on circadian rhythms in animals. The NPs used in our study have a particle size of 200 nm (Fig. 1A). We detected the activity patterns of mice using metabolic cages, and the results demonstrated clear circadian rhythmic activity, characterized by active behavior in darkness followed by a rapid and substantial decline in activity upon entering the light phase (Fig. 1B, C). The robust circadian rhythmic activity observed in the non-NPs-treated group indicates that our experimental system is well-suited for rhythm detection experiments. We treated mice with three concentrations of NPs and analyzed the rhythms of the treated mice separately (Fig. S1). In the 0.1 $\mu\text{g}/\text{mL}$ NPs-treated group, the locomotion patterns of the two groups of mice were nearly identical (Fig. 1C). Comparisons of activity levels between the dark and light phases did not reveal significant differences (Fig. S2). In the treatment group exposed to 1 $\mu\text{g}/\text{mL}$ NPs, mice tended to reduce activity during the dark phase and increased activity during the light phase; however, these differences were not statistically significant (Fig. 1D). When the NPs concentration was elevated to 10 $\mu\text{g}/\text{mL}$, the addition of NPs to drinking water did not influence the water intake of the mice (Fig. S3). The treatment group demonstrated a significant decrease in activity during the dark phase and a significant increase in activity during the light phase (Fig. 1E-G). This result was further

corroborated in a long-time, multi-period rhythmic assay (Fig. 1H). Mice treated with 10 $\mu\text{g}/\text{mL}$ NPs displayed dysrhythmia across multiple consecutive light cycles. Statistical analysis across these cycles indicated that NPs exposure diminished the activity amount difference between the dark and light phases compared to the control group (Fig. 1I, J). The median ratio of the relative activity of mice decreased from 3.1 to 1.5 (Fig. 1J). However, is this change attributable to the inhibition of locomotor ability in the mice due to NP treatment? We compared the total amount of locomotor activity of the mice across each group and found no significant differences (Fig. S4). The total amount of exercise was unchanged, but the difference between diurnal and nocturnal activity was decreasing, suggesting that NP exposure disrupts rhythmicity in mice. Collectively, the difference between dark-phase and light-phase activity in the mice gradually diminished as the concentration of NP treatment increased, suggesting that NP exposure induced a rhythmic disturbance in neuromodulation.

3.2. Identification of NPs in SCN in brain

After 200 nm NPs exposure, plastics were detected in several regions of the mouse brain, including the cortex, hippocampus, and hypothalamus (Zou et al., 2024; Liang et al., 2024; Zhang et al., 2024). We hypothesized that the circadian rhythmic disorders observed in mice following NP exposure may be attributed to the infiltration of NPs into brain regions responsible for rhythm regulation, thereby disrupting their normal function. The suprachiasmatic nucleus (SCN), a critical rhythm-regulating region, is located in the hypothalamus at the base of the brain (Dibner et al., 2010). We detected the contents of plastics in this specific area of brain tissue and compared it with that in the cortex (Fig. 2A). We utilized a mouse model specifically expressing a fluorescent probe (GCaMP6f) in GABAergic neurons within the SCN as a reference for sampling (Fig. 2A). The results indicated an accumulation of NPs in the SCN, with NPs levels increasing in relation to exposure concentration. Notably, there was no significant difference in NPs levels between the SCN and cortex (Fig. 2B). This finding suggests that NPs can access the SCN and may influence mouse rhythmicity by affecting the function of SCN brain regions. We did not assess NPs accumulation in other brain regions or in other tissues and organs; however, previous studies have indicated the potential for such accumulation (Liang et al., 2024; Zhang et al., 2024). Based on the data from the 1 $\mu\text{g}/\text{mL}$ and 10 $\mu\text{g}/\text{mL}$ NPs treatment groups, the detection values in the SCN were not linear. We speculate that the 0.1 $\mu\text{g}/\text{mL}$ NPs treatment group also possesses a significant potential for NPs accumulation.

The regulation of circadian rhythms is a complex network that encompasses both the core biological clock and the biological clocks of peripheral organs. Therefore, the potential role of NPs in initiating this

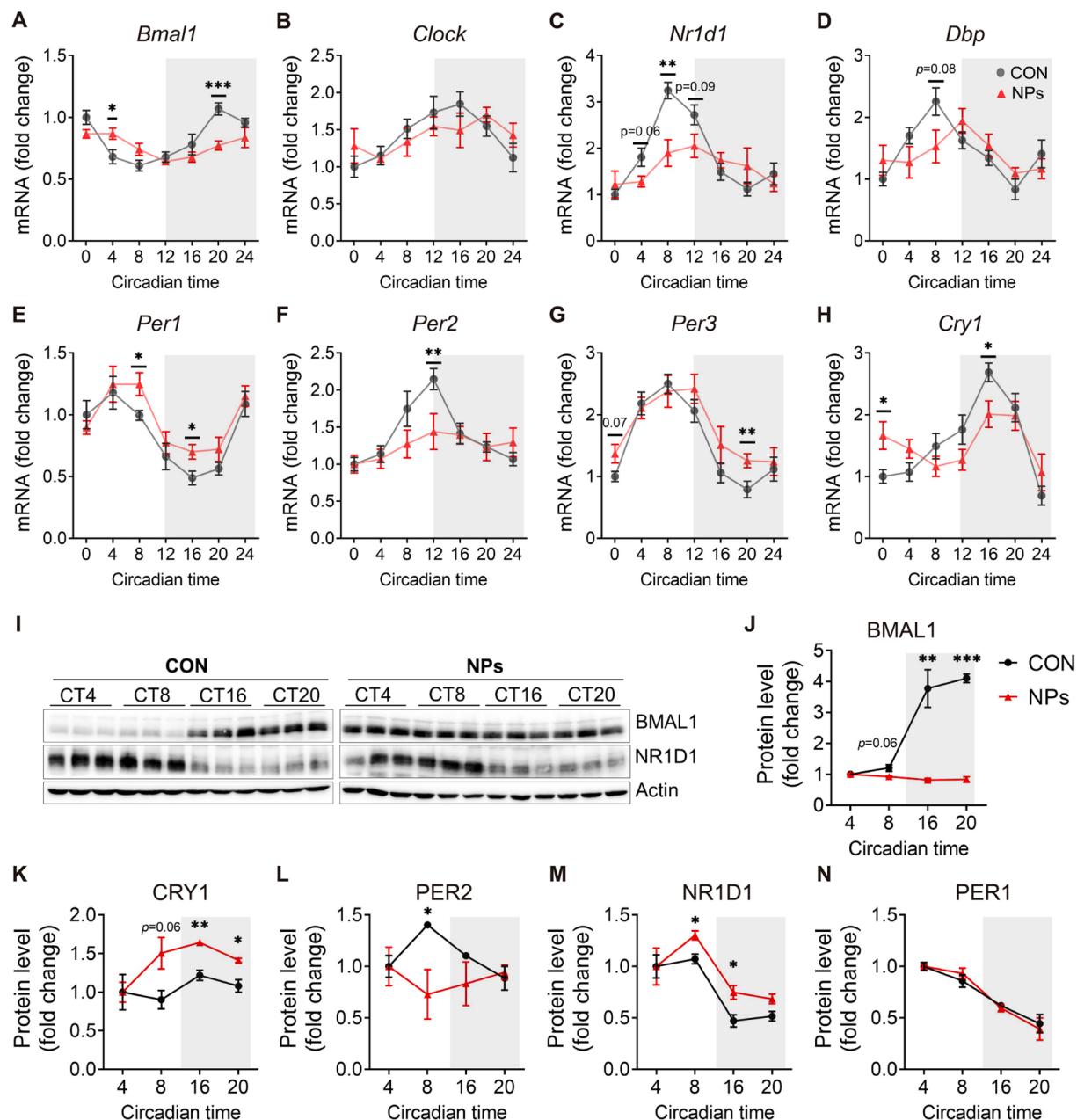


Fig. 3. NPs influence the expression of circadian clock genes in the SCN. (A-H) Expression levels of the core circadian clock genes in the SCN at different time points ($n = 5-6$ for each group). (I) Western blot analysis was conducted to assess the protein levels of BMAL1 and NR1D1 in the SCN. (J-N) Quantitative analysis of the protein levels of circadian regulators was conducted, with data from different time points for each group normalized to CT 4 of the group. Data are represented as mean \pm SEM. * $P < 0.05$, ** $P < 0.01$, *** $P < 0.001$.

rhythmic regulatory network in other organs should not be overlooked. The accumulation of NPs in the SCN may significantly impact the core rhythm regulator.

3.3. NPs influence the expression of circadian clock genes in the SCN

The regulation of rhythmic information by the SCN is contingent upon the regular oscillations of circadian rhythm-regulated genes (Hastings et al., 2018). These oscillations, facilitated through transcriptional regulation and post-translational modifications, establish a coordinated and unified network of gene activity that generates oscillatory fluctuations on a 24-hour cycle (Hastings et al., 2018, Herzog et al., 2017). The rhythmic signals are exported from the core biological clock, the SCN, and transmitted to peripheral rhythmic tissues, collectively regulating the physiological rhythmic behaviors of animals (Froy,

2011).

To investigate whether NPs influence the rhythmic oscillations of the core biological clock, we examined the fluctuations of rhythm-regulated genes in the SCN (Fig. S5). Significant variances in expression levels were noted among six out of the nine core genes associated with the circadian clock that were examined (Fig. 3A-H, Fig. S6). *Bmal1* serves as an essential initiator of rhythmicity, orchestrating the activation of other rhythmic gene oscillations. Notably, the circadian clock gene *Bmal1* exhibited a significant increase in expression induced by NPs at CT4 and a marked suppression at CT20 (Fig. 3A). The changes in *Bmal1* expression influenced by NPs may account for the suppression of activity during the dark phase, and the enhancement of activity during the light phase in mice (Hastings et al., 2018). Circadian clock genes *Nr1d1*, *Per2*, and *Cry1* demonstrated that the gene expression levels at their peak during the 24-hour oscillation cycle were suppressed by NPs (Fig. 3C, F,

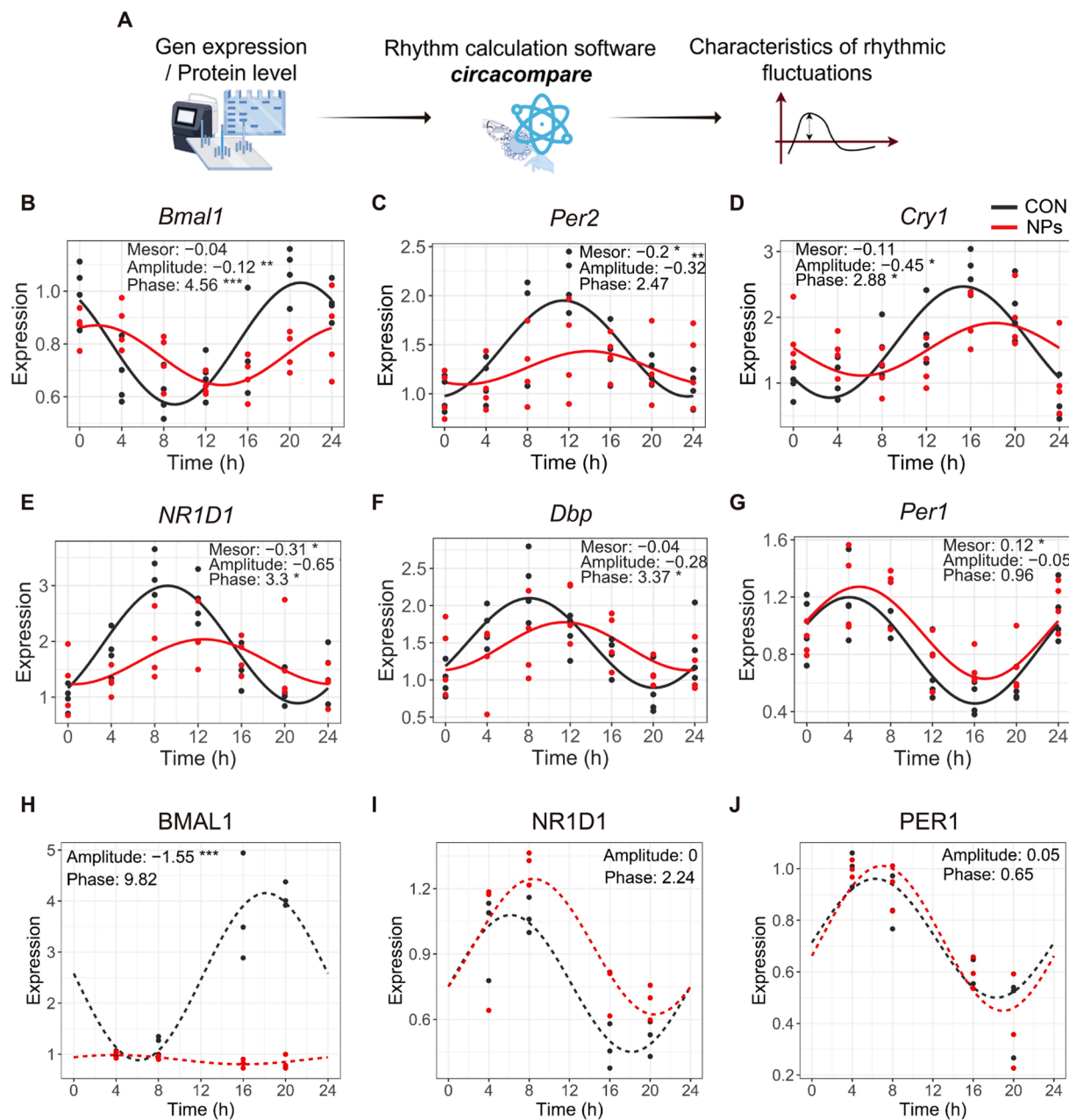


Fig. 4. Regular fluctuations of core circadian clock genes were disrupted by NPs. (A) Overview of the characteristic analysis of fluctuations in circadian rhythm regulators. (B–J) The circadian rhythm oscillation analysis software, Circacompare, was utilized to examine the fluctuation characteristics of the rhythm genes (B–G) and proteins (H–J) influenced by NPs. * $P < 0.05$, ** $P < 0.01$, *** $P < 0.001$.

H). However, following its peak at CT4, the circadian clock gene *Per1* displayed an elevated expression level due to NPs (Fig. 3E). However, the expression levels of *Clock*, *Dbp*, and *Cry2* were not significantly influenced by NPs (Fig. 3B, D, Fig. S6).

Subsequently, we endeavored to identify alterations in the protein levels of the core circadian clock genes, successfully detecting 5 proteins (Fig. 3I, Fig. S7). We quantified these circadian clock proteins and normalized the results with the CT4 values for each group to account for relative fluctuations. Similar with the gene expression levels, NPs also inhibited the increase in BMAL1 protein levels after the onset of the dark cycle (Fig. 3J). NPs induced inverse fluctuations in CRY1 and PER2 protein levels from CT4 to CT8 compared to the control group (Fig. 3K, L). Additionally, NPs resulted in a greater fluctuation in NR1D1 protein levels from CT4 to CT8, while the overall trend remained consistent (Fig. 3M). No significant change was observed in the fluctuation of PER1

protein levels (Fig. 3N). Corresponding to the transcriptional regulatory network, circadian clock regulation also encompasses a tightly controlled set of translational regulation and post-translational modification networks. Our results suggest that NPs exposure not only affects the transcriptional regulation of circadian clock genes but may also impact other regulatory levels, influencing protein level fluctuations, particularly with respect to the core circadian clock-regulating protein BMAL1.

3.4. Regular fluctuations of core circadian clock genes were disrupted by NPs

To systematically and comprehensively evaluate the effects of NPs on circadian clock gene fluctuations, we employed circacompares, a computational tool designed for this purpose, to analyze the

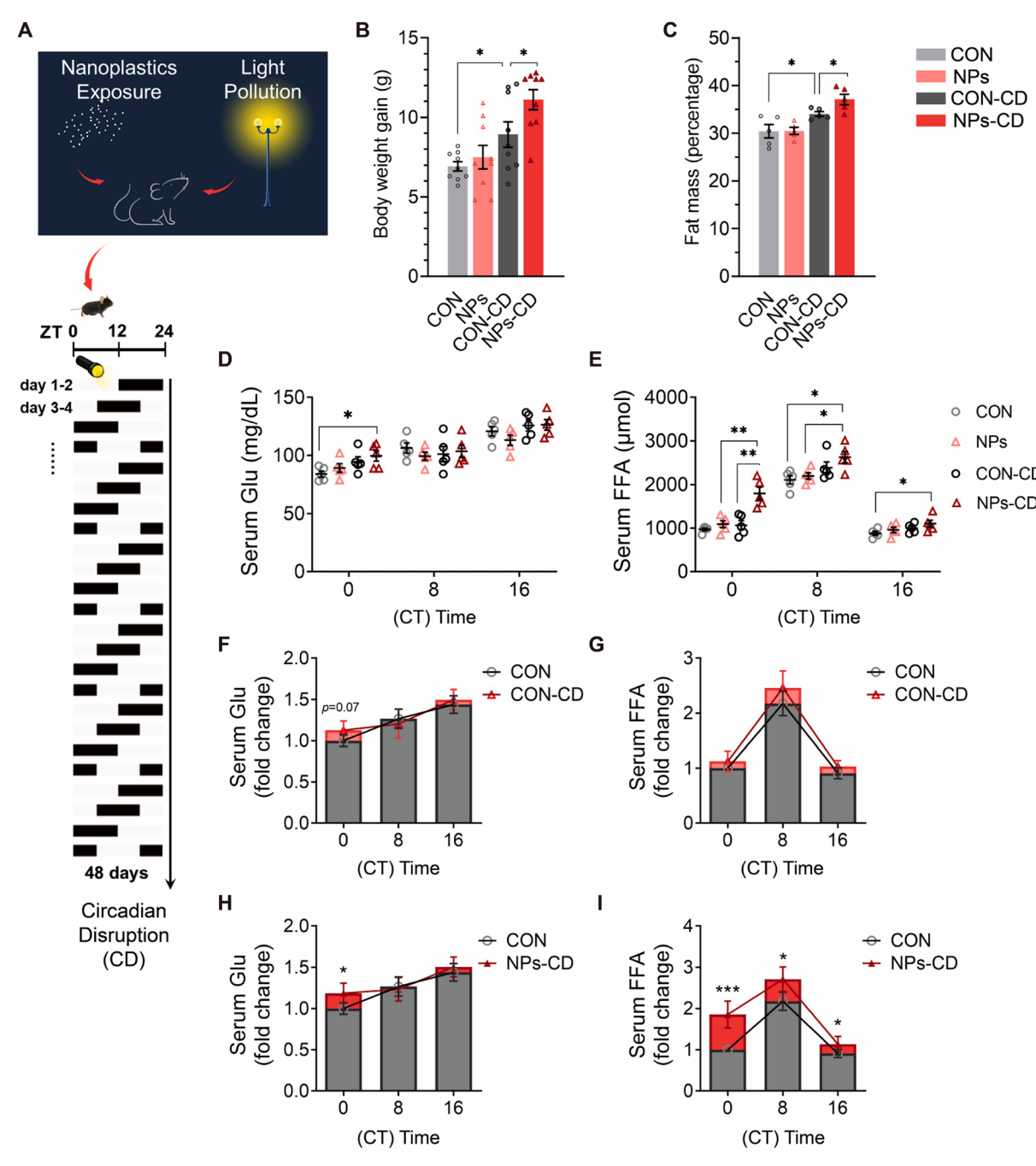


Fig. 5. NPs exacerbate metabolic abnormalities in light pollution exposure. (A) Schematic depiction of the light pollution and NPs induced circadian disruption. (B) Body weight gain of mice ($n = 9$ mice for each group). (C) Measurement of body fat content ($n = 5$ mice for each group). (D, E) Measurement of the serum glucose (D) and free fatty acids (E) at different time points ($n = 5$ mice for each group). (F, G) Relative fold changes of the CON-CD group compared to the CON group at indicated time points were assessed, with data from different time points for each group normalized to CT 0 of the CON group. (H, I) Relative fold changes of the NPs-CD group compared to the CON group at indicated time points. Data are represented as mean \pm SEM. * $P < 0.05$, ** $P < 0.01$, *** $P < 0.001$.

characteristics of circadian gene oscillations in both the CON and NPs groups (Fig. 4A). We assessed and compared the mesor, amplitude, and phase of fluctuating gene expression (Reid et al., 2019) (Fig. 4B-G). The results indicated that NPs significantly influenced the amplitude and phase of *Bmal1* and *Cry1* fluctuations (Fig. 4B, D). Additionally, the mesor and amplitude of *Per2* and *Nr1d1* were notably suppressed (Fig. 4C, E), while significant phase changes were observed in *Nr1d1* and *Dbp* (Fig. 4E, F). However, the amplitude and phase of *Per1*, *Per3*, *Cry2*, and *Clock* did not exhibit significant changes (Fig. 4G, Fig. S8). In terms of protein level fluctuations, a significant inhibition of amplitude was

exclusively observed in *BMAL1* (Fig. 4H-J, Fig. S9).

Overall, these results suggest that NPs can influence the fluctuation of circadian clock genes in the SCN, as evidenced by the inhibition and phase effects on gene vibration amplitude. Both the transcription and protein levels of BMAL1 are concurrently affected by NPs, leading to a reduction in fluctuation amplitude. This finding is consistent with the results of our rhythm detection experiments conducted on mice (Fig. 1G). Consequently, these findings indicate that NPs can disturb the temporal regulatory function of the SCN as a core circadian clock, potentially contributing to physiological rhythm disorders in mice

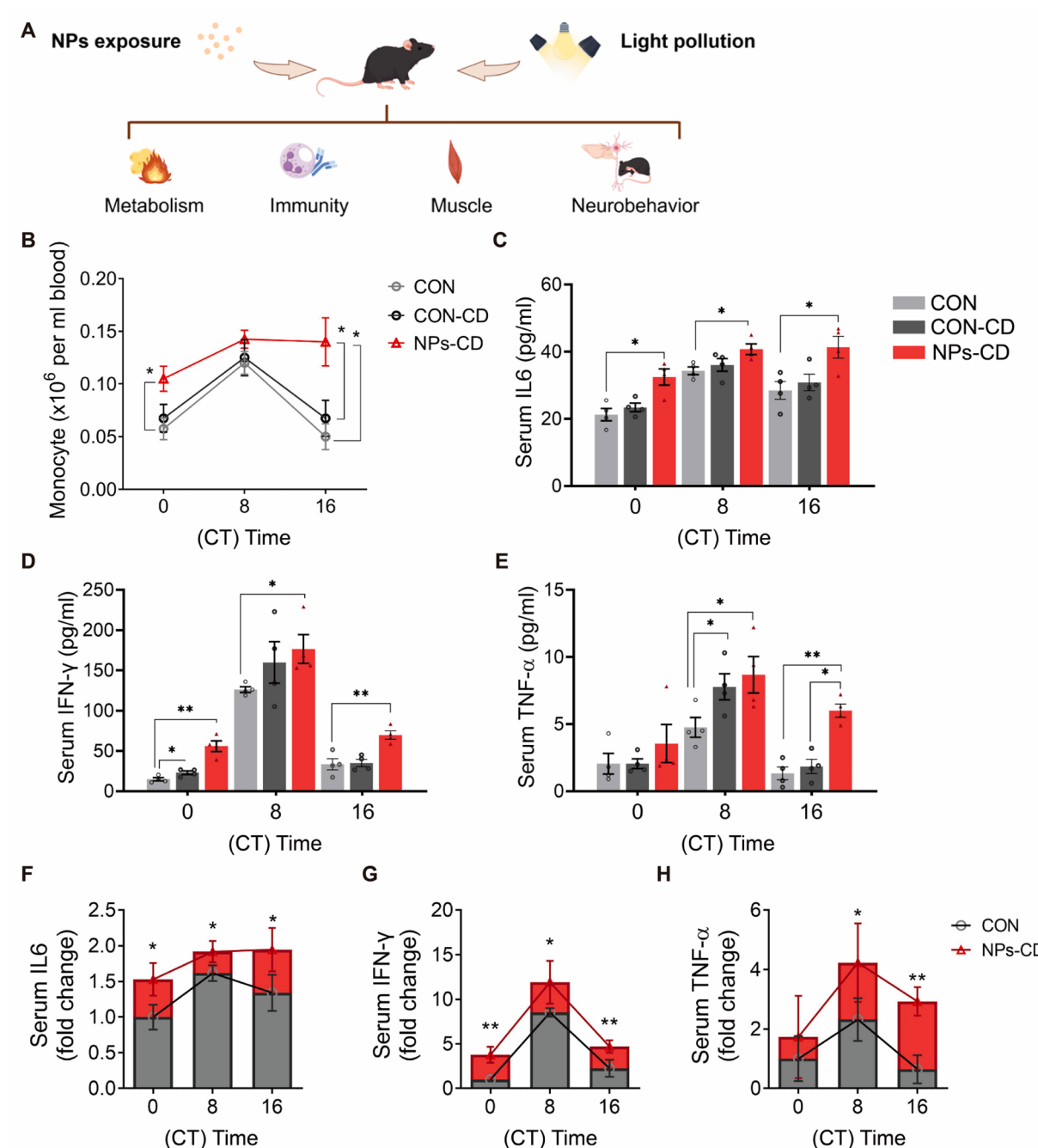


Fig. 6. Immunity disorders induced by NPs in light pollution exposure. (A) Physiological functions that may be impacted. (B) Fluctuations in blood monocyte levels. (C-E) Measurement of the serum immune factor levels, IL6 (C), IFN- γ (D) and TNF- α (E). (F-H) Relative fold changes of the NPs-CD group compared to the CON group at indicated time points were assessed, with data from different time points for each group normalized to CT 0 of the CON group. Data are represented as mean \pm SEM. * $P < 0.05$, ** $P < 0.01$.

exposed to NPs. However, NPs can accumulate in organs other than the brain, leading to dysfunction. Consequently, the physiological rhythm disorders influenced by NPs may also be regulated by other organs.

3.5. NPs exacerbate metabolic abnormalities in light pollution exposure

Among the three NP exposure concentrations we established, only the highest concentration of 10 μ g/mL caused significant physiological rhythm disturbances in mice. However, it is noteworthy that, although the statistical analysis did not reveal a significant difference, exposure to 1 μ g/mL NPs similarly induced a trend of rhythmic changes (Fig. 1D). Like the 10 μ g/mL treatment group (Fig. 1E), mice exposed to 1 μ g/mL

exhibited a trend towards decreased activity during the dark phase and increased activity during the light phase. These findings suggest that exposure to 1 μ g/mL NPs also rendered the regular activity rhythms of the mice more precarious and fragile, potentially increasing their susceptibility to perturbation. Additionally, plastic was detected in SCN tissues exposed to 1 μ g/mL NPs, albeit at lower levels than those in tissues exposed to 10 μ g/mL NPs (Fig. 2B). This could account for the differences in the performance of the two groups of mice in the rhythm assay.

It is important to note that the excessive use of artificial light sources contributes to light pollution, which adversely affects the human living environment. This disruption results in a deviation from the ideal cycle

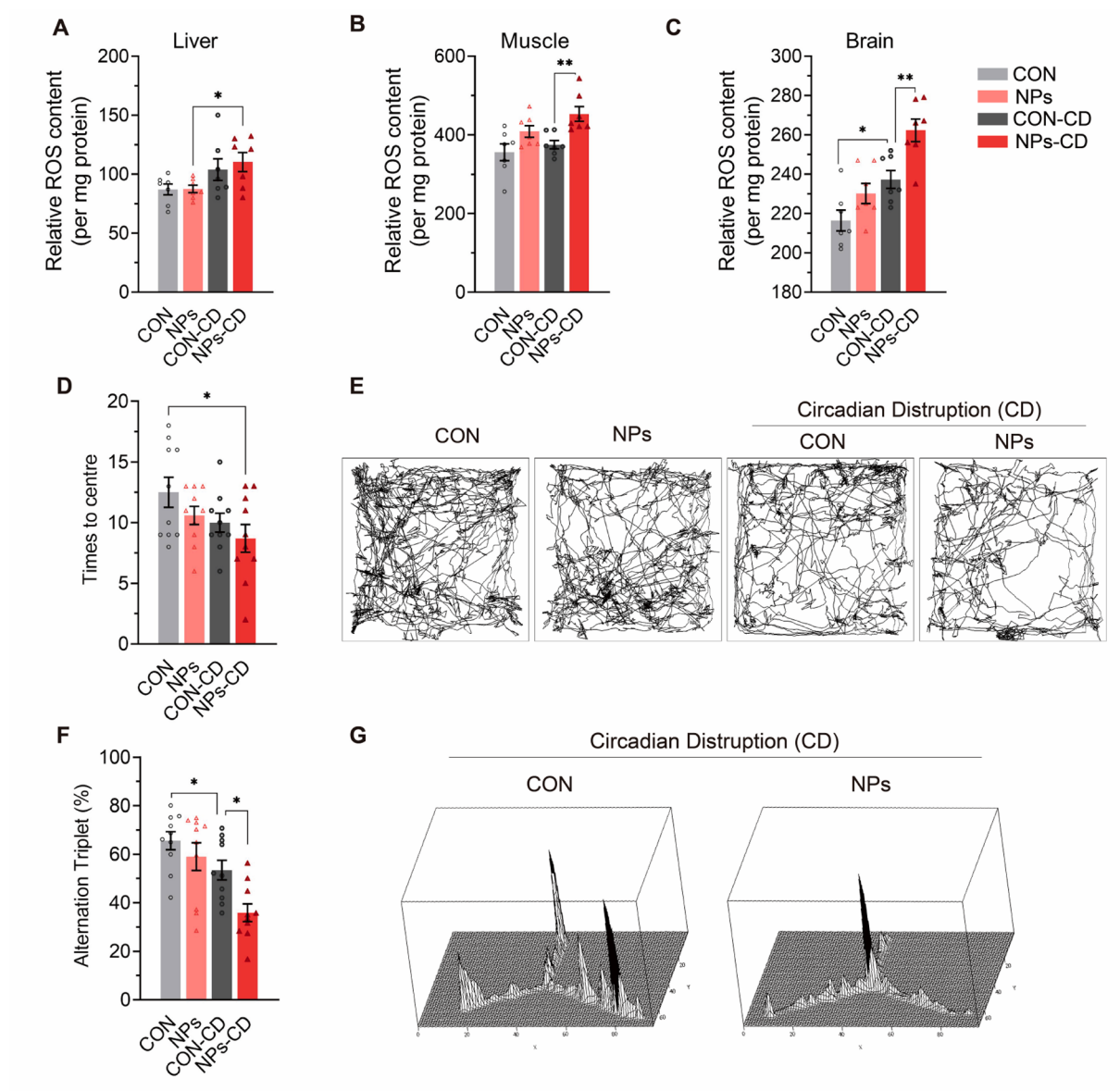


Fig. 7. Higher ROS accumulation in the brains of NPs mice accompanied by abnormalities in neurological function. (A-C) ROS levels in tissues, liver (A), and brain (C). (D, E) Open field test, times mice entered the center zone ($n = 9-10$) (D), representative mice movement trajectory diagrams in the open field test (E). (F, G) Y maze experiment, analytical statistics of the alternation triplet, representative mice movement trajectory diagrams in the Y maze test (G). Data are represented as mean \pm SEM. * $P < 0.05$, ** $P < 0.01$.

of 12 h of light and 12 h of darkness that characterizes a 24-hour day. Light pollution has emerged as a distinct category of environmental pollutants, particularly prevalent in urban settings. It disrupts the regulation of the human circadian clock and physiological rhythms, posing a significant threat to human health. Thus, urban populations are especially vulnerable, facing compounded challenges from both microplastic pollution and ambient light pollution. To investigate the health effects of this dual hazard, we conducted experiments involving mice exposed to NPs while simultaneously subjected to light pollution (Fig. S10), as illustrated in Fig. 5A.

We selected a treatment concentration of 1 $\mu\text{g}/\text{mL}$ NPs for the experiment. After approximately seven weeks of exposure to light pollution, the circadian rhythms of both control and NP-exposed mice were significantly disrupted (Fig. S11A), with the NP-exposed mice showing more severe disruptions (Fig. S11B). We named these two light pollution treatment groups as circadian disruption (CD) groups. Considering that physiological rhythms can directly regulate metabolism, particularly lipid metabolism, we assessed the body weight and

fat content of the mice. Both CD groups exhibited increased body weight (Fig. 5B, Fig. S12). However, the NP-exposed mice experienced a more substantial weight gain, due to increased fat accumulation (Fig. 5C). Furthermore, NP-exposed mice demonstrated elevated levels of blood glucose and lipids at various time points post CD-treatment (Fig. 5D, E). In particular, at CT0, the levels of serum free fatty acids (FFAs) in the NPs-CD exposed groups were significantly higher than those in the control groups (Fig. 5E). As illustrated in Fig. 5F, G indicated that CD treatment had a certain effect compared to the CON, although this effect was not statistically significant. NPs induced a more pronounced impact on metabolism following CD treatment, leading to significant alterations in glucose and FFA levels, particularly in CT0 (Fig. 5H, I). Moreover, the regular fluctuations in FFA levels were disrupted (Fig. S13), indicating that the rhythmic regulation of lipid metabolism was impaired.

3.6. Immunity disorders induced by NPs in light pollution exposure

Next, we intend to investigate the effects of NPs-CD exposure in three

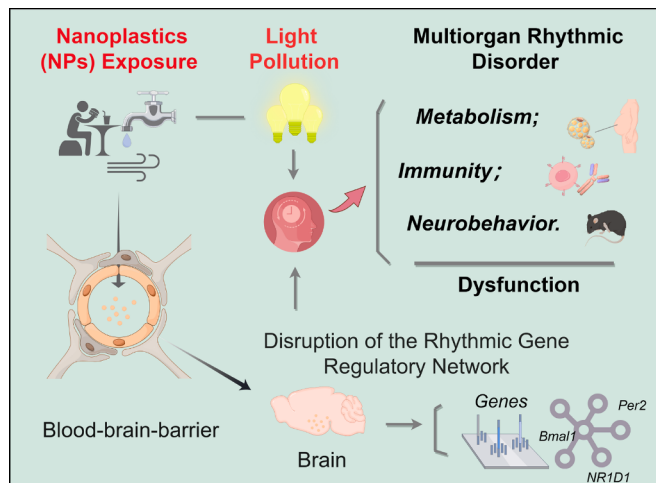


Fig. 8. Schematic Representation of the NPs Induced Multiorgan Disorders in Light Pollution Exposure: NPs in the environment can enter organisms through diet and drinking water, subsequently penetrating the bloodstream. Their small size allows them to cross the blood–brain barrier and infiltrate brain tissues, including the SCN. NPs can disrupt the circadian gene regulatory network, thereby affecting the regulation of the SCN, which serves as the central biological clock. This disruption can lead to the dysregulation of rhythms and functions in peripheral organs that are governed by the biological clock.

additional domains: immune regulation, muscle strength, and neurobehavioral activity (Fig. 6A). The immune system is rhythmically regulated by the biological clock. Maintaining rhythmic immune homeostasis is vital for overall health, particularly in regulating inflammatory responses and combating pathogen invasion. We assessed blood monocyte and immune factor levels at various time points. The untreated control group exhibited significant fluctuations in blood monocyte levels (Fig. 6B). In contrast, the NPs-CD-exposed group demonstrated marked upregulation of monocyte levels at both CT0 and CT16 (Fig. 6B), indicating hyperactivation of immune responses, as no downregulation was observed during the suppressed period (CT0 and CT16). Notably, CD alone did not induce significant changes. Similarly, the NPs-CD-exposed group demonstrated an upregulation of immune factors at nearly all detected time points for IL-6 and IFN- γ (Fig. 6C, D), with significantly higher levels observed at CT 8 and CT 16 for TNF- α (Fig. 6E). Compared to NPs-CD, standalone CD notably increased blood IFN- γ levels exclusively at CT0 and augmented blood TNF- α levels at CT8 (Fig. 6E). To illustrate the changes in quantity more clearly, we calculated the relative changes in the levels of immune factors. The results indicated that the NPs-CD treatment led to an overall increase in the levels of immune factors at different time points (Fig. 6F-H). The findings indicate that NPs-CD disrupts the biological clock's regulation of immunity, resulting in a loss of control that manifests as a hyperimmune state at various time points. Furthermore, these findings suggest that the combination of NPs exposure and CD significantly amplifies the effects of light pollution on immune function.

3.7. Higher ROS accumulation in the brains of NPs mice accompanied by abnormalities in neurological function

Rational regulation of circadian rhythms facilitates organisms' health in undergoing cycles of work and sleep, which are essential for detoxifying harmful substances from the body and mitigating the accumulation of damage signals such as reactive oxygen species (ROS) (Logan and McClung, 2019). Disturbances in these rhythms can lead to mood disorders and memory impairments. In our subsequent experiments, we investigated whether exposure to NPs diminishes the ability of mice to repair damage following CD. We measured ROS levels in the

liver, muscle, and brain (Fig. 7A-C). ROS levels were significantly elevated in all three organs of the NPs-CD group. Especially in the brain, the NPs-CD group exhibited markedly higher ROS levels compared to control mice exposed to light pollution (Fig. 7C). This indicates that NPs exposure suppresses the brain's ability to mitigate ROS damage when subjected to circadian rhythmic disruption. Additionally, in the emotional-behavioral assessment, only the exploratory behavior of mice in the NPs-CD exposure group was significantly inhibited (Fig. 7D, E). However, there was no difference in the total distance traveled (Fig. S14). In working memory detection, CD resulted in memory impairment in both groups of mice (Fig. 7F, G). Consistent with the brain ROS assay, NPs exposure further exacerbated working memory deficits, leading to significantly lower memory performance in mice compared to the controls, even though the group that also undergoing CD treatment. However, no significant change was found in the detection of muscle grip force (Fig. S15), indicating a specific effect of NPs on the brain.

In this study, we focused exclusively on the changes in circadian clock within the SCN of the brain influenced by NPs. However, the regulation of circadian rhythms involves a synergistic interaction among multiple tissues and organs, and it remains unclear how NPs affect the circadian clocks in other brain regions and peripheral tissues, as well as whether NPs deposited in these tissues influence the expression of circadian clock genes. The SCN serves as the central circadian clock tissue, and the perturbation of rhythms caused by NPs, particularly the impact on the core circadian clock gene *Bmal1* (Fig. 3A, J, Fig. 4B, H), is likely to significantly disrupt the circadian clock system. Furthermore, light pollution directly affects the SCN, and when compared to the CD group, the NPs-CD group exhibited notably exacerbated physiological dysregulation and rhythmic damage (Fig. 5I, Fig. 6B, Fig. 7A-C), indicating that the influence of NPs in the SCN is critical.

Among the three NPs exposure concentrations we established, no changes in circadian rhythms were observed in the mice within 0.1 μ g/mL NPs exposure group. However, when the exposure concentration was increased to 1 μ g/mL NPs (a tenfold increase), it compromised the robustness of circadian homeostasis and markedly heightened the organism's susceptibility to light pollution-induced effects, resulting in more severe organ dysfunction. A recent analysis of plastic levels in human organs revealed brain concentrations of 5000 μ g (MPs)/g (brain tissue) (Campen et al., 2024), which exceeds the levels of plastic found in the brain tissue of our treated mice. This finding underscores the alarming extent of continued environmental plastic pollution exposure for humans. The impact of NPs on our brains may extend beyond previously understood.

Our findings underscore the importance of considering that the health effects of NPs exposure in humans may be compounded by physiological rhythm disturbances induced by environmental light pollution, thereby exacerbating the threat to human health. Nonetheless, further *in vitro* and *in vivo* studies are necessary to elucidate the underlying biological mechanisms and to establish causality, contributing to a better understanding of the enhanced damage by NPs in light-induced circadian disruption.

4. Conclusion

Overall, we demonstrated that NPs can invade the SCN in the brain, where the core circadian clock is located, and disrupt the rhythmic regulation of core biological clock genes, leading to rhythmic disorders in mice (Fig. 7). For the first time, we simulated human exposure to light pollution while conducting experiments on NPs exposure. Exposure to NPs at concentrations comparable to human levels can exacerbate light pollution-induced physiological rhythm disturbances, including abnormal metabolic regulation and immune hyperactivation. Moreover, NPs exposure can intensify intra-tissue damage following rhythmic disorders in organisms, resulting in neurobehavioral abnormalities in the brain and impaired memory.

CRediT authorship contribution statement

Haipeng Huang: Writing – review & editing, Writing – original draft, Supervision, Project administration, Methodology, Investigation, Conceptualization. **Jiaqi Hou:** Writing – review & editing, Writing – original draft, Resources, Funding acquisition. **Yilie Liao:** Writing – review & editing, Validation, Supervision, Investigation. **Jing Yu:** Methodology. **Beidou Xi:** Writing – review & editing, Supervision, Project administration, Conceptualization.

Declaration of competing interest

The authors declare that they have no known competing financial interests or personal relationships that could have appeared to influence the work reported in this paper.

Acknowledgments

This research was supported by the Fundamental Research Funds for the Central Public-interest Scientific Institution (Grant 2022YSKY-34), and the National Natural Science Foundation of China (51908524). We thank the technicians in the Charles River Laboratory Animal Research Center for their assistance with animal experiments, and the PKU-Nanjing Institute of Translational Medicine for generously sharing reagents and providing access to instruments. The authors sincerely thank all of the volunteers and nurses who participated in this study.

Appendix A. Supplementary material

Supplementary data to this article can be found online at <https://doi.org/10.1016/j.envint.2025.109338>.

Data availability

Data will be made available on request.

References

- Banerjee, A., Shelver, W.L., 2021. Micro- and nanoplastic induced cellular toxicity in mammals: a review. *Sci. Total Environ.* 755 (Pt 2), 142518.
- Campen, M., Nihart, A., Garcia, M., Liu, R., Olewine, M., Castillo, E., Bleske, B., Scott, J., Howard, T., Gonzalez-Estrella, J., Adolphi, N., Gallego, D., Hayek, E.E., 2024. Bioaccumulation of microplastics in decedent human brains assessed by pyrolysis gas chromatography-mass spectrometry. *Res Sq. rs.3.rs-4345687*.
- Caو, M., Xu, T., Yin, D., 2023. Understanding light pollution: recent advances on its health threats and regulations. *J. Environ. Sci. (China)* 127, 589–602.
- Dibner, C., Schibler, U., Albrecht, U., 2010. The mammalian circadian timing system: organization and coordination of central and peripheral clocks. *Annu. Rev. Physiol.* 72, 517–549.
- Ding, Y., Zhang, R., Li, B., Du, Y., Li, J., Tong, X., Wu, Y., Ji, X., Zhang, Y., 2021. Tissue distribution of polystyrene nanoplastics in mice and their entry, transport, and cytotoxicity to GES-1 cells. *Environ. Pollut.* 280, 116974.
- Froy, O., 2011. The circadian clock and metabolism. *Clin. Sci. (Lond.)* 120 (2), 65–72.
- Gigault, J., Halle, A.T., Baudrimont, M., Pascal, P.Y., Gauffre, F., Phi, T.L., El Hadri, H., Grassl, B., Reynaud, S., 2018. Current opinion: what is a nanoplastic? *Environ. Pollut.* 235, 1030–1034.
- Hastings, M.H., Maywood, E.S., Brancaccio, M., 2018. Generation of circadian rhythms in the suprachiasmatic nucleus. *Nat. Rev. Neurosci.* 19 (8), 453–469.
- Herzog, E.D., Hermanstyne, T., Smylie, N.J., Hastings, M.H., 2017. Regulating the suprachiasmatic nucleus (SCN) circadian clockwork: interplay between cell-autonomous and circuit-level mechanisms. *Cold Spring Harb. Perspect. Biol.* 9 (1) a027706.
- Huang, H., Wei, F., Qiu, S., Xing, B., Hou, J., 2023. Polystyrene microplastics trigger adiposity in mice by remodeling gut microbiota and boosting fatty acid synthesis. *Sci. Total Environ.* 890, 164297.
- Hussain, K.A., Romanova, S., Okur, I., Zhang, D., Kuebler, J., Huang, X., Wang, B., Fernandez-Ballester, L., Lu, Y., Schubert, M., Li, Y., 2023. Assessing the release of microplastics and nanoplastics from plastic containers and reusable food pouches: implications for human health. *Environ. Sci. Tech.* 57 (26), 9782–9792.
- Jeong, B., Baek, J.Y., Koo, J., Park, S., Ryu, Y.K., Kim, K.S., Zhang, S., Chung, C., Dogan, R., Choi, H.S., Um, D., Kim, T.K., Lee, W.S., Jeong, J., Shin, W.H., Lee, J.R., Kim, N.S., Lee, D.Y., 2022. Maternal exposure to polystyrene nanoplastics causes brain abnormalities in progeny. *J. Hazard. Mater.* 426, 127815.
- Jiang, W., Kim, B.Y., Rutka, J.T., Chan, W.C., 2008. Nanoparticle-mediated cellular response is size-dependent. *Nat Nanotechnol.* 3, 145–150.
- Karatsoreos, I.N., Bhagat, S., Bloss, E.B., Morrison, J.H., McEwen, B.S., 2011. Disruption of circadian clocks has ramifications for metabolism, brain, and behavior. *PNAS* 108 (4), 1657–1662.
- Larcombe, A.N., Wang, K.C.W., Phan, J.A., Berry, L.J., Noble, P.B., 2019. Confounding effects of gavage in mice: impaired respiratory structure and function. *Am. J. Respir. Cell Mol. Biol.* 61 (6), 791–794.
- Liang, B., Huang, Y., Zhong, Y., Li, Z., Ye, R., Wang, B., Zhang, B., Meng, H., Lin, X., Du, J., Hu, M., Wu, Q., Sui, H., Yang, X., Huang, Z., 2022. Brain single-nucleus transcriptomics highlights that polystyrene nanoplastics potentially induce Parkinson's disease-like neurodegeneration by causing energy metabolism disorders in mice. *J. Hazard. Mater.* 430, 128459.
- Liang, B., Deng, Y., Zhong, Y., Chen, X., Huang, Y., Li, Z., Huang, X., Yang, X., Du, J., Ye, R., Xian, H., Feng, Y., Bai, R., Fan, B., Yang, X., Huang, Z., 2024. Gastrointestinal incomplete degradation exacerbates neurotoxic effects of PLA microplastics via oligomer nanoplastics formation. *Adv. Sci.* 11 (28).
- Lin, S., Zhang, H., Wang, C., Su, X.L., Song, Y., Wu, P., Yang, Z., Wong, M.H., Cai, Z., Zheng, C., 2022. Metabolomics reveal nanoplastic-induced mitochondrial damage in human liver and lung cells. *Environ. Sci. Tech.* 56 (17), 12483–12493.
- Liu, Z., Sokratian, A., Duda, A.M., Xu, E., Stanhope, C., Fu, A., Strader, S., Li, H., Yuan, Y., Bobay, B.G., Sipe, J., Bai, K., Lundgaard, I., Liu, N., Hernandez, B., Bowes Rickman, C., Miller, S.E., West, A.B., 2023. Anionic nanoplastic contaminants promote Parkinson's disease-associated α -synuclein aggregation. *Sci. Adv.* 9 (46), eadi8716.
- Logan, R.W., McClung, C.A., 2019. Rhythms of life: circadian disruption and brain disorders across the lifespan. *Nat. Rev. Neurosci.* 20 (1), 49–65.
- Lu, Y.Y., Li, H., Ren, H., Zhang, X., Huang, F., Zhang, D., Huang, Q., Zhang, X., 2022. Size-dependent effects of polystyrene nanoplastics on autophagy response in human umbilical vein endothelial cells. *J. Hazard. Mater.* 421, 126770.
- Miguelena Chamorro, B., Swaminathan, G., Mundt, E., Paul, S., 2023. Towards more translatable research: exploring alternatives to gavage as the oral administration route of vaccines in rodents for improved animal welfare and human relevance. *Lab Anim (NY)* 52 (9), 195–197.
- Mohamed Nor, N.H., Kooi, M., Diepens, N.J., Koelmans, A.A., 2021. Lifetime accumulation of microplastic in children and adults. *Environ. Sci. Tech.* 55 (8), 5084–5096.
- Parsons, R., Parsons, R., Garner, N., Oster, H., Rawashdeh, O., 2020. CircaCompare: a method to estimate and statistically support differences in mesor, amplitude and phase, between circadian rhythms. *Bioinformatics* 36 (4), 1208–1212.
- Pastore, C., 2021. Size-dependent nano-bio interactions. *Nat. Nanotechnol.* 10, 1052.
- Reid, K.J., 2019. Assessment of circadian rhythms. *Neurol. Clin.* 37 (3), 505–526.
- Rillig, M.C., Lehmann, A., 2020. Microplastic in terrestrial ecosystems. *Science* 368 (6498), 1430–1431.
- Senathirajah, K., Attwood, S., Bhagwat, G., Carbery, M., Wilson, S., Palanisami, T., 2021. Estimation of the mass of microplastics ingested - a pivotal first step towards human health risk assessment. *J. Hazard. Mater.* 404 (Pt B), 124004.
- Smolensky, M.H., Sackett-Lundeen, L.L., Portaluppi, F., 2015. Nocturnal light pollution and underexposure to daytime sunlight: complementary mechanisms of circadian disruption and related diseases. *Chronobiol. Int.* 32 (8), 1029–1048.
- Tähkämö, L., Partonen, T., Pesonen, A.K., 2019. Systematic review of light exposure impact on human circadian rhythm. *Chronobiol. Int.* 36 (2), 151–170.
- Vethaak, A.D., Legler, J., 2021. Microplastics and human health. *Science* 371 (6530), 672–674.
- Wright, S.L., Kelly, F.J., 2017. Plastic and human health: a micro issue? *Environ. Sci. Tech.* 51 (12), 6634–6647.
- Ze, Y., Sheng, L., Zhao, X., Ze, X., Wang, X., Zhou, Q., Liu, J., Yuan, Y., Gui, S., Sang, X., Sun, Q., Hong, J., Yu, X., Wang, L., Li, B., Hong, F., 2014. Neurotoxic characteristics of spatial recognition damage of the hippocampus in mice following subchronic peroral exposure to TiO₂ nanoparticles. *J. Hazard. Mater.* 264, 219–229.
- Zhang, J., Peng, M., Lian, E., Xia, L., Asimakopoulos, A.G., Luo, S., Wang, L., 2023. Identification of poly (ethylene terephthalate) nanoplastics in commercially bottled drinking water using surface-enhanced raman spectroscopy. *Environ. Sci. Tech.* 57 (22), 8365–8372.
- Zhang, Z., Chen, W., Chan, H., Peng, J., Zhu, P., Li, J., Jiang, X., Zhang, Z., Wang, Y., Tan, Z., Peng, Y., Zhang, S., Lin, K., Yung, K.K., 2024. Polystyrene microplastics induce size-dependent multi-organ damage in mice: insights into gut microbiota and fecal metabolites. *J. Hazard. Mater.* 461, 132503.
- Zielinska-Dabkowska, K.M., Schernhammer, E.S., Hanifin, J.P., Brainard, G.C., 2023. Reducing nighttime light exposure in the urban environment to benefit human health and society. *Science* 380 (6650), 1130–1135.
- Zou, L., Xu, X., Wang, Y., Lin, F., Zhang, C., Liu, R., Hou, X., Wang, J., Jiang, X., Zhang, Q., Li, L., 2024. Neonatal exposure to polystyrene nanoplastics impairs microglia-mediated synaptic pruning and causes social behavioral defects in adulthood. *Environ. Sci. Tech.* 58 (27), 11945–11957.